Int. J. Heat Mass Transfer, Vol. 25, No. 1, pp. 45–55, 1982.
Printed in Great Britain

0017-9310/82/010045-11 $03.00/0

BOILING IN LOW-PERMEABILITY POROUS MATERIALS

HAIM H. BAU* and K. E. TORRANCE
Sibley School of Mechanical and Aerospace Engineering, Cornell University, Ithaca, NY 14853, U.S.A.

(*Received* 27 *January* 1981 *and in revised form* 19 *May* 1981)

Abstract—Experimental observations are reported on boiling in a vertical circular cylinder heated from below and cooled from above. The cylinder is filled with low-permeability, water-saturated porous materials. With the onset of boiling an almost isothermal, 2-phase (wet steam) zone forms near the bottom. This zone is overlain by a liquid layer with an essentially linear vertical temperature gradient. The temperature field in the overlying liquid layer is oscillatory whenever the height of the 2-phase zone exceeds a critical value. A simple 1-dim. model is used to predict the height of the 2-phase zone, the dry-out heat flux, and a necessary condition for the formation of a 2-phase zone.

NOMENCLATURE

c_p, specific heat;
d, average grain diameter of bed material;
D, diameter of porous bed, Fig. 1;
F, relative permeability, see equations (5) and (11);
g, acceleration of gravity;
H, height of porous bed, Fig. 1;
H_v, height of vapor zone, Fig. 8;
$H_{2\phi}$ height of 2-phase zone, Fig. 8;
h_{lv} latent heat of vaporization;
k_e, effective thermal conductivity of saturated porous bed;
$\dot{m}$, mass flow per unit area;
p, pressure;
q, heat flux per unit area;
q_{max}, maximum heat flux per unit area across two-phase zone;
Ra Rayleigh number, defined in equation (2);
Ra_b, Ra value at onset of boiling, defined in equation (15);
Ra_c, critical Ra value at onset of single-phase convection;
S, saturation (fraction of pore volume occupied by liquid phase);
T, temperature;
T_b, temperature at bottom of bed;
T_o, temperature at top of bed;
T_{sat}, saturation or boiling temperature;
ΔT, temperature difference;
z, vertical coordinate.

Greek symbols

β, volume thermal expansion coefficient;
Γ, non-dimensional heat flux, defined in equation (8);
λ, permeability, see equation (1);
ν, kinematic viscosity;
ρ, density;
ϕ, porosity of bed.

Subscripts

f, fluid property;
l, liquid property;
v, vapor property.

1. INTRODUCTION

BOILING in porous media can occur in many contemporary engineering applications, such as geothermal systems, heat pipes, post-accident analyses of liquid-cooled nuclear reactors, and nuclear waste disposal. Although the relevant literature is growing, uncertainties exist about many aspects of the boiling process. For example, various experiments on boiling with heating from below have suggested that adjacent to the heating surface there exists a thin liquid layer [1], a vapor layer [2], or a layer with both vapor and liquid regions [3].

Experimental studies [4–6] also report the formation of an isothermal 2-phase zone above the bottom whenever the bottom temperature exceeds saturation. In such a 2-phase zone, heat transfer can occur only by a convective process. Visualization techniques have been used to study the flows. Sondergeld and Turcotte [5] report cellular convection patterns in the 2-phase zone in an experiment with bottom heating. The cells interacted with the liquid zone overlying the 2-phase zone. Lee and Nilson [6] report cellular convection in the overlying liquid, but did not observe convection cells in the 2-phase zone. They did however observe a vertical countercurrent flow of vapor and liquid in the 2-phase zone. Their experiments employed volumetric heating. A 1-dim. 2-phase Darcy flow model has been used to model heat transfer and dry-out conditions in the 2-phase zone [4–6].

*Present Address: Department of Mechanical Engineering and Applied Mechanics, University of Pennsylvania, Philadelphia, PA 19104, U.S.A.

fluidizing), water-saturated porous beds. The apparatus is a closed circular cylinder heated from below and cooled from above. The upper and lower boundaries are isothermal. The top of the cylinder is permeable. The phrase "low-permeability" is used to emphasize that prior to the onset of boiling convection does not occur. That is, the appropriate layer Rayleigh numbers are subcritical. Temperature measurements are reported for a range of heating rates. A 1-dim. model is used to describe the heat transfer in the 2-phase zone. A dry-out heat flux is predicted at which an isothermal 2-phase layer transforms to a vapor layer. The model is also used to obtain a necessary condition for the formation of a 2-phase zone. This explains the previous disagreement over the vapor or liquid–vapor character of the layer adjacent to the heating surface [2, 3]. Unstable oscillatory flows are observed when the height of the 2-phase zone exceeds a critical value.

2. EXPERIMENTAL APPARATUS AND PROCEDURE

The experimental apparatus is shown schematically in Fig. 1. The apparatus consists of an inner Pyrex tube of inner diameter $D = 9.5$ cm and an outer, coaxial, stainless steel tube (17.8 cm I.D.). Both tubes are 31.8 cm high and are sealed at the bottom to a brass plate (1.3 cm thick). Two cavities are formed in this way. The inner cavity is a vertical, circular cylinder; the outer cavity is a vertical, annular cylinder. The inner cavity is used as the test region; the outer cavity forms an insulating thermal guard.

The inner and outer cavities are filled to the same height with water-saturated permeable media. The water is distilled and degassed. Brass plates (1.3 cm thick) with O-ring seals are placed on top of the porous bed. The plates are perforated (3.2 mm holes on 1.3 cm centers) to allow throughflow and are covered with a screen (40 meshes/cm) to contain the porous media. The height of the bed, H, can be varied. The porous media is tamped to aid settling and the top plates are pressed downward with mechanical screw-jacks to prevent fluidization of the bed. A water layer of 3–5 cm is maintained above the perforated plates. The apparatus is placed on an isothermal hot plate (1 cm thick aluminum) using a thermally-conducting grease seal and the apparatus is levelled. The two compartments at the top are cooled by passing tap water through separate copper coils located above the brass top plates. The open top is sealed with a plastic sheet to minimize evaporation. The entire rig is wrapped with a (1.5 cm thick) layer of fibreglass insulation.

The cooling-water temperature rise and flow rate are measured with a thermopile and a rotameter, respectively. These measurements allow the heat flow through the system to be calculated. As a check, the heat flux is compared to the conductive heat flux using known reference materials in the cavities. The agreement is to within $\pm$ 20%. A network of 36 gauge copper–constantan thermocouples is embedded at various locations within the porous material. (A typical arrangement is shown in Fig. 5.) Temperatures are recorded continuously with a multichannel strip

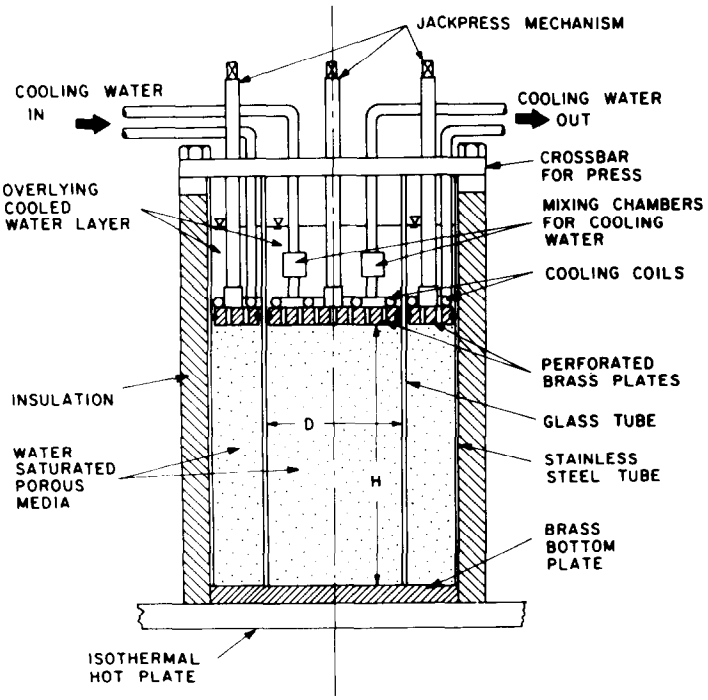

FIG. 1. Schematic diagram of the experimental apparatus.

chart recorder and may also be displayed on a digital voltmeter. Further details are available in reference [7].

Commercially-available granular materials are used for the permeable beds. They include two types of Pyrex glass beads and a silica sand as listed in Table 1. The porosity (ϕ) is measured experimentally to $\pm$ 2% by displacing water as a bed is packed, and the permeability (λ) is obtained from the Kozeny–Carman formula [8, p. 166]

$$\lambda = \frac{d^2}{180} \frac{\phi^3}{(1-\phi)^2} \quad (1)$$

where d is the average grain diameter. Note that the two types of glass beads with similar mean diameters ($d = 0.110$ and 0.105 mm) have very different permeabilities. The bed with the wider range of grain sizes has a lower porosity and permeability. The effective thermal conductivity of the fluid-saturated porous medium, k_e, is found by applying a known temperature gradient and measuring the heat flux while in a conductive regime.

Experiments are carried out by starting from a quiescent initial state. The heating rate at the lower boundary is changed in a sequence of very small steps. After each step a period of several hours is allowed in order to achieve steady-state.

Preliminary experiments revealed that a small amount of soluble material in the Pyrex or silica beads would go into solution over time scales of several weeks (the lifetime of an experiment). When boiling occurred the dissolved material was deposited near the heating surface. The result was a cementing of the matrix, a locally-reduced permeability, and higher heating-surface temperatures. In extreme cases an almost impermeable crust (2 cm thick) was formed next to the heater. We found that cementation could be eliminated by adding a small amount of buffer solution (pH 7) to the distilled water in the experiment. Buffering appears to have a negligible effect on fluid properties. Cementation was also observed by Schrock *et al.* [9] in boiling experiments with silica sand. The cementation was found to be cementaceous $CaSO_4$ and $CaCO_3$, and was attributed to the use of tap water.

3. EXPERIMENTAL RESULTS

Experimental measurements include the temperature field within, and the vertical heat flux across, the inner cylinder shown in Fig. 1. Results are reported for the three beds listed in Table 2. Each bed was packed with a particular granular material to a height, H, or bed aspect ratio, H/D. Other entries in the table will be discussed in the next section.

Centerline temperature profiles are shown in Figs. 2, 3(a) and 4(a). Each figure corresponds to a different bed material. The curve parameter is the heat flux through the bed. Linear temperature profiles are observed up to the onset of boiling. This confirms the dominance of conduction and the absence of convection.

When the bottom temperature achieves the saturation temperature of $T_{sat} = 100°C$, an almost isothermal zone forms above the bottom in Figs. 2(a), 3(a) and 4(a). This zone is at essentially the saturation temperature. It is a 2-phase, wet-steam zone in which liquid and vapor can coexist. Heat is presumably transferred through this zone by a vertical countercurrent flow of liquid and vapor which will be described in the next section. The bottom superheat at the onset of the 2-phase boiling process was observed to be less then 1K in all cases. This is less than the 8K super heat observed in pool boiling [10, p. 7] and may be explained in terms of the porous matrix providing additional nucleation sites, poor convective cooling of vapor sites, and good

Table 1. Physical properties of granular bed materials

Material and supplier	Mean grain diameter, d (mm)	Diameter range (mm)	Porosity, ϕ	Permeability, λ (10^{-12}m^2)	Thermal conductivity, k_e (W/m K)
MS-M glass beads (Cataphote-Ferro)	0.110	0.74–0.149	0.37	8.5	0.92
Braun glass beads (Braun Melsungen)	0.105	0.10–0.11	0.40	11	0.96
Silica sand S-151 (Fisher Scientific)	0.254	0.21–0.31	0.40	64	2.60

Table 2. Geometry, Rayleigh numbers, and q_{max} for three water-saturated porous beds

Mean grain diameter of bed material, d (mm)	Bed height (cm)	Height/diameter of bed, H/D	Ra_c	Ra_b	Predicted q_{max} (kW/m^2)
0.110	18.7	1.97	71.3	2.24	4.2
0.105	15.9	1.67	54.6	2.36	9.2
0.254	21.7	2.28	88.6	6.91	53.0

thermal contact between the heating surface and any bubbles.

The temperature profile in the liquid layer overlying the 2-phase zone is essentially linear in Figs. 2(a), 3(a) and 4(a). Only in the case of the most permeable bed [Fig. 4(a)] is there an observable departure from linearity (shown by dashed lines). Since the profiles are basically linear, it is unlikely that convection could account for more than 20–30% of the total heat transfer. Temperature measurements made away from the centerline reveal that the isotherms are essentially horizontal in both the 2-phase and overlying liquid zones. For the case of the most permeable bed, however, there is a slight tilting of the isotherms away from the horizontal in the liquid layer at high heat flows. Nevertheless, the overall heat flow is predominantly vertical and one-dimensional.

Figure 2 illustrates the effect of cementation by comparing the boiling process in two beds of the same material ($d = 0.105$ mm beads) and of the same height. The left and right graphs correspond to beds without cementation and with cementation, respectively. The profiles for the case with cementation [Fig. 2(b)] do not display an isothermal 2-phase zone. Instead, temperatures in the low-permeability cementation region near the bottom are above 100°C and indicate a dry steam zone. The differences in the boiling structure between Figs. 2(a) and 2(b) are due entirely to alterations in the bed. By controlling the pH of the water, other results presented in this paper are free of cementation effects. By way of contrast, cementation occurred in the experiments of Sondergeld and Turcotte [4] and may account for the dry steam zones which they observed.

The height of the 2-phase zone increases with the heat flux through the layer, q, as shown in Figs. 3(b)

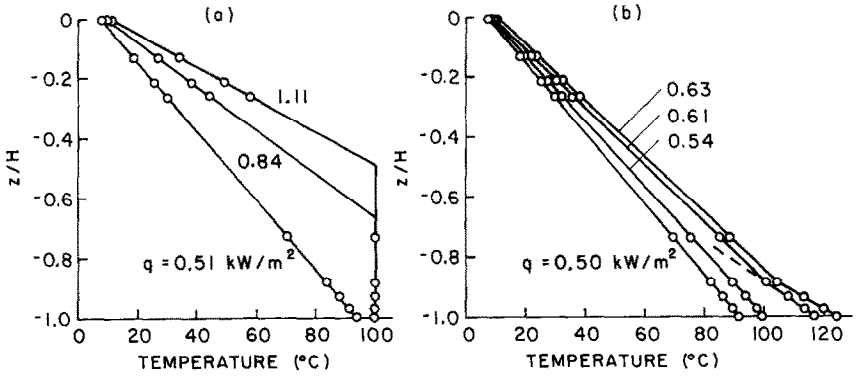

FIG. 2. Centerline temperature profiles illustrating the boiling process in two beds with the same original permeability, $\lambda = 11 \times 10^{-12}$m^2 (grain size $d = 0.105$ mm), and same height. The curve parameter is the heat flux q. (a) A bed free of cementation. (b) A bed with cementation in the lowest 2 cm.

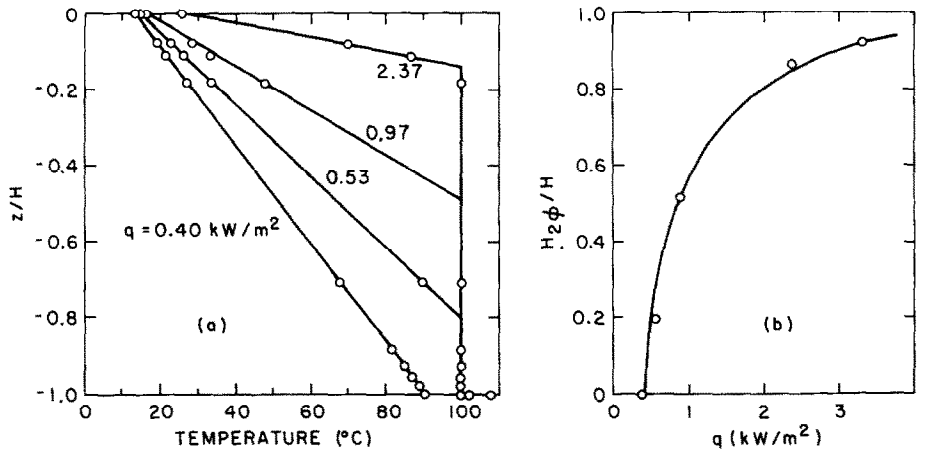

FIG. 3. Experimental results for a porous bed with permeability $\lambda = 8.5 \times 10^{-12}$m^2 (grain size $d = 0.110$ mm). (a) Centerline temperature profiles. (b) Relative height of the 2-phase zone, $H_{2\phi}/H$, as a function of the heat flux q. The solid line is the prediction of equation (13).

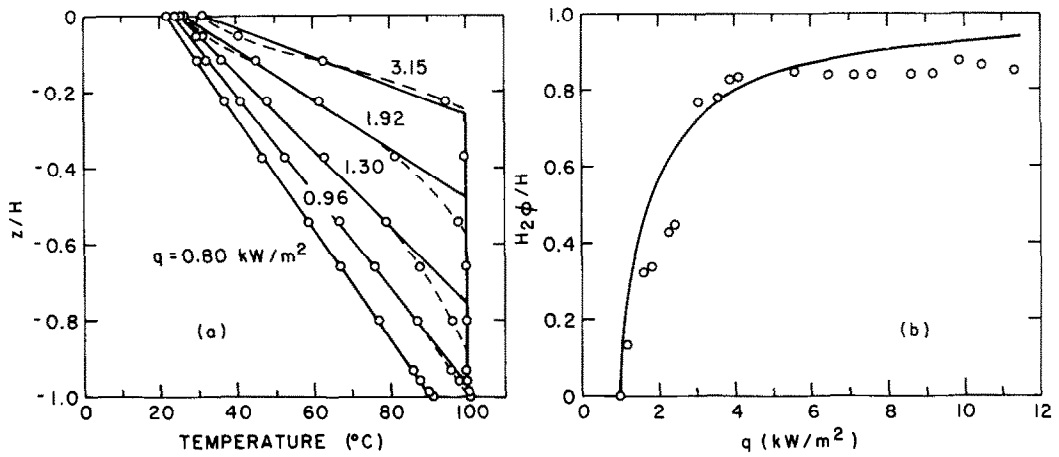

FIG. 4. Experimental results for a porous bed with permeability $\lambda = 64 \times 10^{-12}\text{m}^2$ (grain size $d = 0.254$ mm). (a) Centerline temperature profiles. (b) Relative height of the 2-phase zone, $H_{2\phi}/H$, as a function of the heat flux q. The solid line is the prediction of equation (13).

and 4(b). These figures correspond to the beds of lowest and highest permeability, respectively. The open circles represent experimental data. The solid lines denote an analytical result to be discussed later.

When the height of the 2-phase zone is less than about 70–80% of the bed height the temperature field in the overlying water zone is observed to be time steady or stationary. Above this value, time-periodic oscillations are observed in the water temperature and in the measured heat flux. The oscillations observed with the most permeable bed are shown in Figs. 6 and 7. Thermocouple locations are identified in Fig. 5. Figures 6 and 7 correspond to mean vertical heat flows of $q = 7.5\,\text{kW/m}^2$ and $8.7\,\text{kW/m}^2$, respectively. Figure 6 reveals that the thermocouples in the overlying water zone oscillate in phase with a period of about 900 s. Thermocouples S, W, O, N and E are located in the same horizontal plane. Thermocouple U is above this plane, thermocouples T_1 and T_2 are mounted at the top of the bed, and thermocouple B is mounted on the heating surface. The oscillations also undergo a long period fluctuation in amplitude which has a period of about three hours in Fig. 7. Both the long-period fluctuations and the short-period oscillations were found to be independent of bed loading by varying the screwjack pressure on the bed (see Fig. 1). They are thus not attributable to fluidization of the bed.

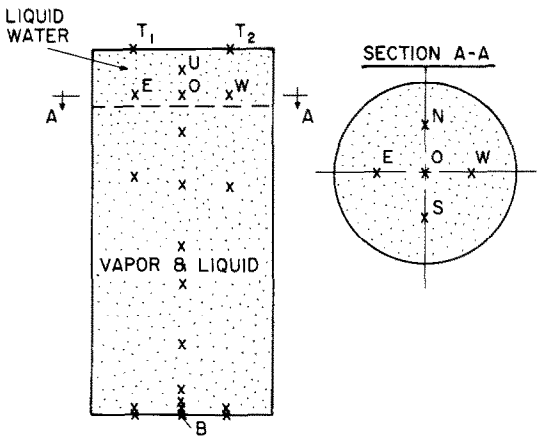

FIG. 5. Schematic diagram of a water-saturated porous bed. Thermocouple locations (the x's) correspond to the temperature transients shown in Figs. 6 and 7. The dashed line indicates the approximate height of the 2-phase zone.

4. ANALYSIS AND DISCUSSION

The preceding section reported experimental data on heat transfer across a vertical circular cylinder of height H and diameter D which was heated from below and cooled from above. The cylinder was filled with porous media of low permeability so that single-phase thermal convection was inhibited. Temperature profiles revealed the dominance of conduction heat transfer and the emergence of an isothermal 2-phase zone in which water and steam coexisted.

A systematic analysis of the experimental results is presented in this section. Use will be made of the conceptual 1-dim. model shown in Fig. 8. The model consists of three layers: an overlying liquid–water layer, an intermediate 2-phase, vapor–liquid layer, and a possible underlying vapor layer. The latter is included for discussion purposes although it was not observed in the present experiments. The height of the liquid/2-phase interface is denoted by $H_{2\phi}$; the height of the vapor layer is denoted by H_v. Planar interfaces are assumed between the layers.

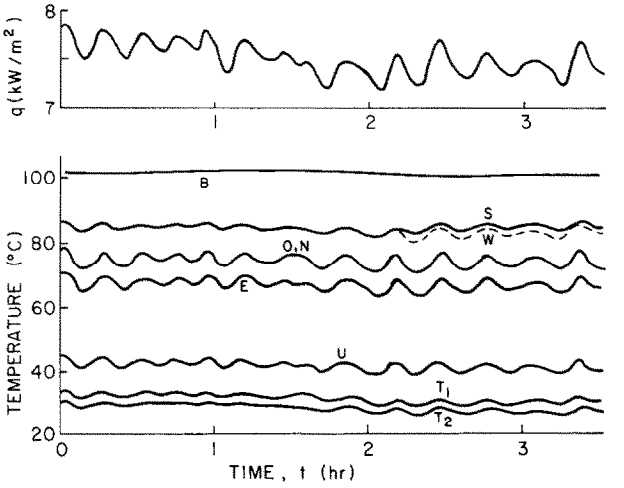

FIG. 6. Temperature and heat flux transients for a porous bed with permeability $\lambda = 64 \times 10^{-12}\text{m}^2$ (grain size $d = 0.254$ mm). The mean heat flux is 7.5 kW/m^2. Thermocouple locations are shown in Fig. 5.

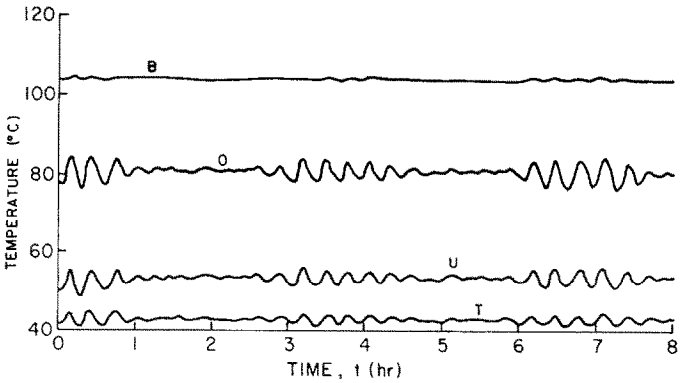

FIG. 7. Temperature transients for a porous bed with permeability $\lambda = 64 \times 10^{-12}\text{m}^2$ (grain size $d = 0.254$ mm). The mean heat flux is 8.7 kW/m^2. Both short term oscillations and long term fluctuations are visible. Thermocouple locations are shown in Fig. 5.

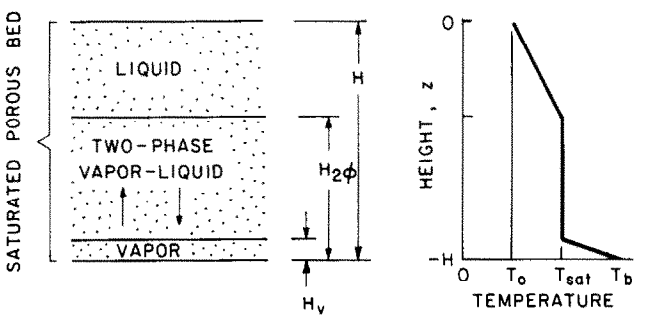

FIG. 8. Schematic diagram of the 1-dim. boiling model. The model applies to low-permeability, saturated beds. Planar interfaces are assumed between the various zones.

4.1. *Subcritical convective state*

We first examine the conditions under which single-phase thermal convection might be expected to develop.

The onset of convection in a cylinder of fluid-saturated porous material with a permeable top and an impermeable bottom, both of which are isothermal, has been analyzed by Bau and Torrance [11]. The Rayleigh number for a single-phase permeable layer of height H is defined by

$$Ra = \frac{g\lambda\beta_f \Delta T H}{\nu_f (k_e/\rho_f c_{pf})}. \quad (2)$$

Subscripts f and e denote properties of the fluid and the fluid-saturated porous matrix, respectively. The bottom-to-top temperature difference, $T_b - T_o$, is denoted by ΔT. The value of Ra corresponding to the onset of single-phase convection is referred to as the critical Rayleigh number, Ra_c. Values of Ra_c from [11] are listed in Table 2 and are a function of the cylinder aspect ratio H/D. The Rayleigh number at the onset of boiling in the experiments, Ra_b, is also listed in Table 2. This Rayleigh number is based on the temperature difference $\Delta T = T_{sat} - T_o$ and the layer height H. Clearly, in all cases $Ra_c > Ra_b$. Since Ra_b represents an upper bound on the liquid-layer Rayleigh number, convection prior to the onset of boiling is not expected.

After the onset of boiling, we observe the evolution of a 2-phase zone beneath an overlying liquid layer. Although the Rayleigh number for the overlying liquid layer remains smaller than Ra_c, this fact alone does not guarantee a subcritical convective state for the liquid layer. This follows because Ra_c is a function of the boundary conditions and the lower boundary conditions change when the 2-phase zone develops. The values of Ra_c in Table 2 correspond to an impermeable bottom. For the case of a liquid-saturated porous layer with permeable upper and lower boundaries, Ra_c is zero [12]. For the case of a liquid layer over a 2-phase zone, an approximate analysis which accounts for the lower boundary condition shows that Ra_c, although not zero, is small [13]. The aforementioned analyses apply to horizontally-infinite layers, but suggest that convection could develop in a liquid layer overlying a 2-phase zone. Nevertheless, the measured temperature profiles in Figs. 2–4 strongly indicate that convection in the liquid layer, if it does occur, plays only a minor role. Consequently, in the subsequent analyses we assume that conduction is the dominant mechanism of heat transfer in the overlying liquid layer.

4.2 *The 2-phase zone*

The experimental results and the foregoing discussion support the use of a heat conduction model for single-phase layers of liquid. The experimental results, however, reveal that a 2-phase zone forms above the heating surface when boiling starts. This zone is at the saturation temperature. Heat transfer across such an isothermal zone requires a convective transport process.

Following prior work [4, 14], we assume a 1-dim., vertical, countercurrent flow of liquid and vapor in the 2-phase zone. Vapor is produced by boiling at the heated lower boundary. The vapor percolates upward to the upper boundary of the 2-phase zone where it is condensed by conductive cooling to the overlying water layer. The condensate then trickles downward to the lower boundary and the boiling cycle can start afresh. The countercurrent flow is driven by the density difference between the liquid and vapor phases. The liquid and vapor phases flow in contiguous capillary paths in opposite directions, and there is a dispersed upward flow of vapor and a dispersed downward flow of liquid. Heat transfer occurs by the convection of latent heat, with phase changes occurring at the horizontal boundaries of the 2-phase zone.

Within the 2-phase zone the vertical mass fluxes of liquid ($\dot{m}_l$) and vapor ($\dot{m}_v$) must balance:

$$\dot{m}_l = -\dot{m}_v = -\dot{m}. \quad (3)$$

Applying Darcy's law to each phase we have [8, p. 459]

$$\dot{m}_l = -\frac{\lambda F_l}{v_l}\left(\frac{dp}{dz} + \rho_l g\right)$$

$$\dot{m}_v = -\frac{\lambda F_v}{v_v}\left(\frac{dp}{dz} + \rho_v g\right) \quad (4)$$

where F is the relative permeability of each phase. The relative permeability represents the ratio of cross-sections available for the liquid and vapor flows, has a value between 0 and 1, and is often approximated by the linear forms

$$F_l = S, \quad F_v = 1 - S \quad (5)$$

where S is the liquid saturation. Eliminating the pressure gradient and combining (3) to (5) yields

$$\dot{m} = \frac{S(1-S)\lambda g(\rho_l - \rho_v)}{(1-S)v_l + Sv_v}. \quad (6)$$

In addition, the vertical heat flux per unit area, q, is attributed to the convection of latent heat h_{lv}:

$$q = h_{lv}\dot{m}. \quad (7)$$

Combining (6) and (7) we can define a non-dimensional heat flux by

$$\Gamma = \frac{qv_v}{\lambda h_{lv} g(\rho_l - \rho_v)} = \frac{S(1-S)}{(1-S)\frac{v_l}{v_v} + S}. \quad (8)$$

The non-dimensional heat flux, Γ, is a function of saturation, as shown in Fig. 9. Large values of S correspond to liquid-dominated systems. In that limit, since $v_v/v_l \sim 70$ for water at 100°C [15], (8) reduces to

$$\Gamma = 1 = S. \quad (9)$$

The linear dependence is in agreement with the open circles in Fig. 9 which represent experimental results

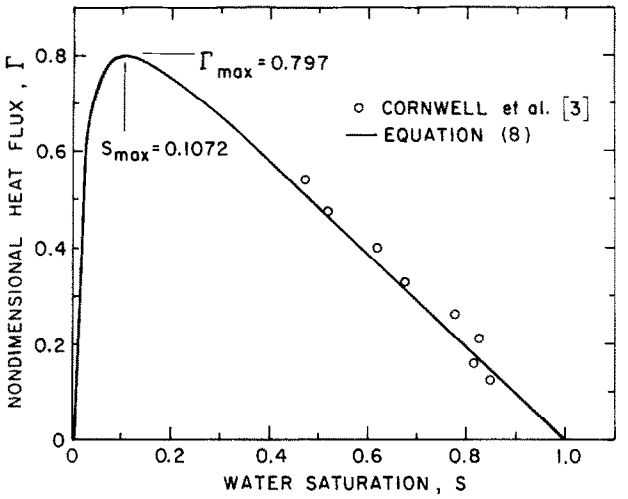

FIG. 9. Comparison of experiment and theory for the boiling of water. The solid curve is the non dimensional heat flux, Γ, predicted by the 1-dim. counterpercolation model [equation (8)].

from Cornwell *et al.* [3]. They measured the boiling heat flux in a saturated porous medium and the areas occupied by liquid and vapor on the heating surface (horizontal). Thus, S represents the fraction of the surface covered by liquid. Another important result of the present analysis is that q is independent of bed height H. This is also supported by experimental observations [1, 16].

4.3. *Maximum heat flux across the 2-phase layer*

The heat flux given by (8) achieves a maximum at a particular value of S, as shown in Fig. 9. The maximum represents the maximum heat flow that can be transported across a 2-phase layer by the counterpercolation mechanism. When the applied heat flux exceeds the maximum, the 2-phase zone in Fig. 8 must disappear and be replaced by a vapor layer. The temperature of the heating surface then jumps to a higher value to support heat conduction across the vapor layer. We thus identify the maximum heat flux (q_{max}) as the dryout heat flux. Differentiation of (8) yields

$$q_{max} = \frac{\lambda h_{lv} g(\rho_l - \rho_v)}{(\sqrt{\nu_l} + \sqrt{\nu_v})^2}. \tag{10}$$

An expression similar to (10) has previously appeared for volumetrically-heated beds [14].

The dry-out heat flux is also independent of bed height, H. This concurs with the dry-out experiments of Dhir and Catton [17] for a volumetrically-heated porous bed. On the other hand, a decrease in the dry-out heat flux with increasing bed height has been reported by Gabor *et al.* [18] and Ferrell and Alleavitch [1] for volumetric and bottom heating. This can be attributed to bed fluidization which decreases with increasing bed height. Nevertheless, the experimental [1, 18] and calculated values of dry-out heat flux are in rough agreement, as shown in Fig. 10. Differences are attributable to bed fluidization and to uncertainties in estimating the bed permeability λ [we used equation (1) for this purpose]. Theoretical estimates of the dry-out heat fluxes for the present experiments are listed in Table 2. We could not confirm the predictions due to limitations in the heat supply in our experiment and to renewed cementation problems in the low-permeability beds at high heat flows.

We also note that the prediction in Fig. 9 is influenced by the form of the relative permeability functions (5). For example, the forms [19]

$$F_l = S^3, \; F_v = 1 - 1.11\,S \tag{11}$$

are often used to describe the drying of partially-saturated soils (some air present). These expressions yield a maximum in Γ of 0.52 at $S = 0.35$, a linear behavior at large S, and a cubic behavior at small S. Nevertheless, the simple linear expressions (5) appear satisfactory because they yield a reasonable fit to the experimental data in Fig. 9.

4.4. *The height of the 2-phase layer*

The location of the upper boundary of the 2-phase zone (see Fig. 8) may be predicted very simply. Since heat conduction dominates in the overlying liquid layer, the heat flux is given by

$$q = k_e \frac{T_{sat} - T_o}{H - H_{2\phi}}. \tag{12}$$

The height of the 2-phase zone is thus

$$\frac{H_{2\phi}}{H} = 1 - k_e \frac{T_{sat} - T_o}{qH}. \tag{13}$$

Clearly, as q increases the thickness of the liquid layer decreases in order to sustain the heat flow. In turn, $H_{2\phi}/H$ increases. The solid lines in Figs. 3(b) and 4(b)

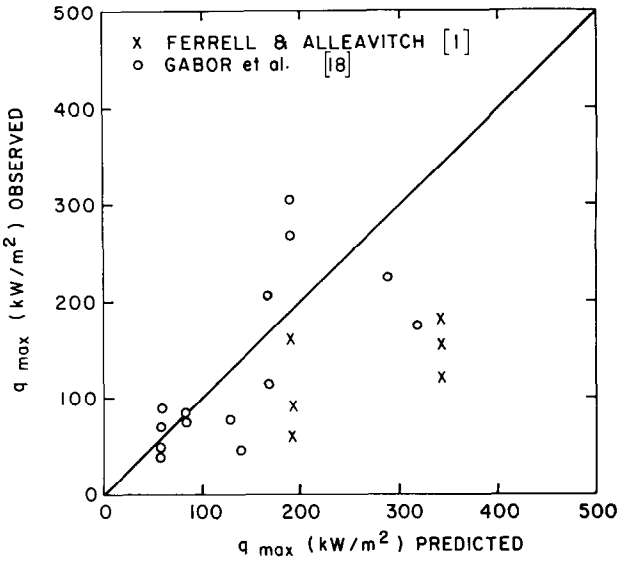

FIG. 10. Comparison of observed values of the dry-out heat flux (q_{max}) for water with values predicted by the counterpercolation model [equation (10)].

represent equation (13), and the agreement with the experimental data is quite reasonable.

A maximum height for the 2-phase zone is predicted when the heat flux reaches the limiting value for a 2-phase layer, q_{max}, from equation (10). In practice the upper bound was not achieved in our experiments. Instead, the oscillatory instability shown in Figs. 6 and 7 developed at $H_{2\phi}/H$ values below the theoretical maximum.

Note that the lower boundary of the 2-phase zone is not predicted. The top boundary is defined by (13) when q is known. With q known, there are two possible values for the saturation S in the zone but, from (8), no constraint on zone thickness. In principle, it is possible to interpose a vapor layer of height H_v below the 2-phase zone (see Fig. 8). The height H_v is indeterminate, but as long as the vapor layer conducts the heat flux q any value in the range $0 \leq H_v \leq H_{2\phi}$ is possible. The corresponding bottom temperature would of course vary from T_{sat} to $T_{sat} + qH_{2\phi}/k_e$ over this range. Such a vapor layer was not observed in the present experiments.

4.5. *Necessary condition for a 2-phase layer*

A 2-phase layer may not always form. Indeed, if the heat flux across the overlying liquid layer at the onset of boiling exceeds the limiting heat flux for a 2-phase zone, then a 2-phase zone cannot develop. Thus, when the inequality

$$k_e \frac{T_{sat} - T_o}{H} > q_{max} \tag{14}$$

is satisfied a vapor layer will form below the liquid layer when boiling starts.

Equation (14) thus yields a necessary (but not sufficient) condition for the formation of a 2-phase layer. Formation of such a zone requires that the liquid-layer heat flux at the onset of boiling be at least less than the limiting heat flux, q_{max}, from equation (10). This inequality yields a necessary condition for the formation of a 2-phase zone in terms of the liquid-layer Rayleigh number at the onset of boiling:

$$Ra_b = \frac{g\lambda\beta_l(T_{sat} - T_o)H}{\nu_l(k_e/\rho_l c_{pl})} > \frac{[1 + \sqrt{(\nu_v/\nu_l)}]^2\beta_l c_{pl}(T_{sat} - T_o)^2}{h_{lv}(1 - \rho_v/\rho_l)}. \tag{15}$$

For the case of water, assuming $T_{sat} - T_o = 100\,K$, this reduces to $Ra_b \gtrsim 0.3$. The value 0.3 is much lower than the Ra_b values in our experiments (Table 2). Hence a 2-phase zone is possible and was observed.

The necessary condition (15) resolves a conflict in the literature. Moss and Kelly [2] observed a vapor layer to form near the heater in their experiments. Other workers [3–6] observed a 2-phase zone. For the experiments of Moss and Kelly [2] we estimate an Ra_b value of less than 0.1. This does not satisfy the inequality in (15). Hence a vapor layer is expected and was observed.

4.6. *Stability of the 2-phase layer*

The appearance of a 2-phase zone raises two interesting stability questions. The first is whether a 2-phase zone will always emerge when the necessary condition (15) is satisfied. Alternative possibilities are a vapor layer or a combination of a 2-phase layer and an underlying vapor layer. Equation (15) is not a sufficient condition for the formation of a 2-phase zone. The second question concerns the gravitational stabi-

lity of a liquid layer overlying a 2-phase zone. As we have seen, theory suggests that convection in the liquid should readily evolve. The experiments do not support this, nor do the experiments reveal any convective overturning of the superposed layers. The foregoing stability questions are only partly resolved by the present study. Furthermore, the present experiments reveal a third kind of instability.

An oscillatory instability (Figs. 6 and 7) develops when the height of the 2-phase zone exceeds 0.7–0.8 of the bed height. The temperature within the liquid above the 2-phase zone oscillates with a period of about 900 s. The entire liquid temperature field oscillates in phase, as if the liquid layer were being physically raised or lowered while the temperature sensors and porous bed remained stationary. Oscillations are observed with other bed materials as well. The oscillatory period appears to be an inverse function of permeability.

Hardee and Nilson [14] reported irregular oscillations of 60–300 s in their boiling experiments. They identified channel venting as the cause. As the bottom temperature rose above saturation, the increased vapor pressure opened channels to the surface which allowed vapor venting. Venting released the pressure and allowed liquid to drain back down. This rewetted the sand, sealed the vapor channels, and lowered the bottom temperature back to saturation. Bed fluidization was thus important. Channeling is an unlikely explanation for the present experiments since the oscillations occur in phase over the entire cross section.

A likely explanation for the present oscillations is the periodic formation and disappearance of a vapor layer next to the heating surface. The associated increase in volume causes an upward movement of the 2-phase zone and the overlying liquid layer. This serves to expel warm fluid across the permeable upper boundary. Eventually the pressure of the vapor increases sufficiently to allow vapor to percolate upward. The bottom area is then rewetted, causing an influx of cool fluid through the upper boundary, and the process starts afresh.

The foregoing explanation leads to a cyclical uplifting of the liquid and 2-phase zones. This is consistent with the transients in Figs. 6 and 7 which show that temperatures in the liquid oscillate essentially in phase.

5. SUMMARY

Experiments are reported for the boiling of water in saturated porous media. Low permeabilities are employed so that the vertical transport of heat is 1-dim. (negligible natural convection circulations). For the case of heating from below and cooling from above (see Fig. 8), we observe the formation of an isothermal 2-phase zone at the onset of boiling. The structure of the zone is described and a necessary condition for its formation is identified. A simple analytical model yields a dry-out heat flux for the 2-phase zone. Above this heat flux a vapor layer replaces the 2-phase zone and there is a jump in the temperature of the heating surface.

Acknowledgements—The authors would like to thank Professor D. L. Turcotte for many helpful discussions. This research has been supported by the Division of Engineering of the National Science Foundation under Grant ENG-7823542.

REFERENCES

1. J. K. Ferrell and J. Alleavitch, Vaporization heat transfer in capillary wick structures, *Chem. Engng Prog. Symp. Ser. No.* 102, **66**, 82–91 (1970).
2. R. A. Moss and A. J. Kelly, Neutron radiographic study of limiting planar heat pipe performance, *Int. J. Heat Mass Transfer* **13**, 491–502 (1970).
3. K. Cornwell, B. G. Nair and T. D. Patten, Observation of boiling in porous media, *Int. J. Heat Mass Transfer* **19**, 236–238 (1976).
4. C. H. Sondergeld and D. L. Turcotte, An experimental study of two-phase convection in a porous medium with applications to geological problems, *J. geophys. Res.* **82**, 2045–2053 (1977).
5. C. H. Sondergeld and D. L. Turcotte, Flow visualization studies of two-phase thermal convection in a porous layer, *Pure appl. Geophys.* **117**, 321–330 (1978).
6. D. O. Lee and R. H. Nilson, Flow visualization in heat-generating porous media, Sandia Report SAND 76-0614, Albuquerque, New Mexico (1977).
7. Haim H. Bau, Experimental and theoretical studies of natural convection in laboratory-scale models of geothermal systems, Ph.D. Thesis, Cornell University, Ithaca, New York (1980).
8. J. Bear, *Dynamics of Fluids in Porous Media*, American Elsevier, New York (1972).
9. V. E. Schrock, R. T. Fernandez and K. Kesavan, Heat Transfer from Cylinders embedded in a liquid filled porous medium, *Heat Transfer 1970*, Vol. VII, Paper CT 3.6, Elsevier, Amsterdam (1970).
10. Y. Y. Hsu and R. W. Graham, *Transport Processes in Boiling and Two-Phase Systems* McGraw-Hill, New York (1976).
11. H. H. Bau and K. E. Torrance, An experimental and analytical study of low Rayleigh number thermal convection in a vertical cylinder filled with porous material, A.S.M.E. Symp. *Natural Convection* (Edited by I. Catton and R. N. Smith) Vol. HTD-16, pp. 17–24 (1981).
12. D. A. Nield, Onset of thermohaline convection in a porous medium, *Water Resources Res.* **4**, 553–560 (1968).
13. G. Schubert and J. M. Straus, Gravitational stability of water over steam in vapor-dominated geothermal systems, *J. geophys. Res.* **85**, 6505–6512 (1980).
14. H. C. Hardee and R. H. Nilson, Natural convection in porous media with heat generation, *Nucl. Sci. Engng* **63**, 119–132 (1977).
15. E. R. G. Eckert and R. M. Drake, *Analysis of Heat and Mass Transfer*. McGraw-Hill, New York (1972).
16. V. I. Krokhin and A. S. Kulikov, Experimental study of boiling heat transfer in liquid nitrogen or helium in capillary-porous bodies, *Heat Transfer—Soviet Research* **10**, 141–146 (1978).
17. V. Dhir and I. Catton, Dryout heat fluxes for inductively heated particulate beds, *J. Heat Transfer* **99**, 250–256 (1977).
18. J. D. Gabor, E. S. Sowa, L. Baker, Jr., and J. C. Cassulo, Studies and experiments on heat removal from fuel debris in sodium, *Fast Reactor Safety Meeting—Los Angeles*, CONF-740401-P2, pp. 823–844. American Nuclear Society (1974).
19. H. G. Botset, Flow of Gas-liquid mixtures through consolidated sands, *Trans. A. I. M. E.* **136**, 91–108 (1940).

EBULLITION DANS DES MATERIAUX POREUX FAIBLEMENT PERMEABLES

Résumé—Des observations expérimentales portent sur l'ébullition dans un cylindre circulaire vertical chauffé à la base et refroidi au sommet. Le cylindre est rempli d'un matériau poreux à faible perméabilité et saturé d'eau. Avec l'apparition de l'ébullition, une zone diphasique (vapeur humide), isotherme se forme vers la base. Cette zone est recouverte par une couche liquide à gradient de température vertical essentiellement linéaire. Le champ de température dans la couche liquide est oscillatoire lorsque la hauteur de la zone diphasique dépasse une valeur critique. Un modèle simple monodimensionnel est utilisé pour prédire la hauteur de la zone diphasique, le flux d'assèchement et une condition nécessaire pour la formation de la zone diphasique.

SIEDEN IN PORÖSEN MATERIALIEN VON GERINGER DURCHLÄSSIGKEIT

Zusammenfassung—Es wird über experimentelle Beobachtungen beim Sieden in einem senkrechten Kreiszylinder berichtet, der von unten beheizt und von oben gekühlt wird. Der Zylinder ist mit wassergesättigten Materialien von geringer Durchlässigkeit gefüllt. Bei Siedebeginn bildet sich am Boden ein fast isothermes Zweiphasen-Gebiet (Naßdampf) aus. Diese Zone ist von einer Flüssigkeitsschicht überlagert, die einen nahezu linearen Temperaturverlauf in senkrechter Richtung aufweist. Das Temperaturfeld in der überlagernden Flüssigkeitsschicht oszilliert, sobald die Höhe des Zweiphasengebiets einen kritischen Wert erreicht. Ein einfaches eindimensionales Modell wird benutzt, die Höhe des Zweiphasengebiets, den Wärmestrom beim Austrocknen und eine notwendige Bedingung für die Ausbildung eines Zweiphasengebiets anzugeben.

КИПЕНИЕ В ПОРИСТЫХ МАЛОПРОНИЦАЕМЫХ МАТЕРИАЛАХ

Аннотация — Представлены результаты экспериментального исследования кипения в вертикальном круглом нагреваемом снизу и охлаждаемом сверху цилиндре, заполненном малопроницаемым пористым материалом, насыщенном водой. С началом кипения у нижней поверхности цилиндра образуется почти изотермическая двухфазная (влажный пар) зона. Непосредственно над этой зоной располагается слой жидкости, характеризующийся в основном линейным вертикальным температурным градиентом. Поле температур в слое колеблется всякий раз, когда высота двухфазной зоны превышает критическое значение. Для расчета высоты двухфазной зоны, критической величины теплового потока и условия, необходимого для образования двухфазной зоны, используется простая одномерная модель.